

Supporting Information

Surface-Functionalizable Amphiphilic Nanoparticles for Pickering Emulsions with Designer Fluid-Fluid Interfaces

Ming Pan,¹ Minkyu Kim,² Lucas Blauch³ and Sindy K. Y. Tang^{2,}*

¹Department of Materials Science and Engineering, Stanford University, Stanford, California
94305-2004, United States

²Department of Mechanical Engineering, Stanford University, Stanford, California 94305-2004,
United States

³Department of Chemical Engineering, Stanford University, Stanford, California 94305-2004,
United States

*Email: sindy@stanford.edu

Table of Contents

Table S1. Detailed reaction conditions for the surface conjugation of NPs

Table S2. Compositions of different phases for droplet generation experiments

Figure S1. Long-term stability of F-SiO₂ NPs synthesized in small scale

Figure S2. XPS spectrum of NH₂-F-SiO₂ NPs with low initial [APTES] synthesized in large scale

Figure S3. AES spectra of 2 μm F-SiO₂ MPs and NH₂-F-SiO₂ MPs

Table S3. Estimation of ratio between surface amine and fluoroalkyl groups on NH₂-F-SiO₂ NPs

Figure S4. Droplet stability tests of F-SiO₂ NPs and NH₂-F-SiO₂ NPs synthesized in large scale

Figure S5. Resorufin leakage test of F-SiO₂ NPs synthesized in large scale.

Figure S6. Resorufin leakage test of NH₂-F-SiO₂ NPs synthesized in large scale

Figure S7. Growth of GFP *E. coli* inside NH₂-F-SiO₂ NPs-stabilized droplets

Figure S8. Growth of *E. coli* K-12 inside NH₂-F-SiO₂ NPs-stabilized droplets

Figure S9. Fluorescence image of droplets stabilized by F-SiO₂ NPs after FITC conjugation
(product obtained from the scheme shown in Fig 2b)

Figure S10. Fluorescence image of droplets stabilized by NH₂-F-SiO₂ NPs pre-incubated with
solid fluorescein in HFE (showing no physical adsorption of fluorescein in NH₂-F-SiO₂ NPs)

Figure S11. Fluorescence image of RB-N-F-SiO₂ NPs stabilized drops in HFE

Figure S12. Fluorescence image of $\text{RB}_{\text{ads}}\text{-F-SiO}_2$ NPs stabilized drops in HFE before and after incubation (with line scan profile)

Figure S13. Scaling plot: % fluorescent NPs VS normalized fluorescence intensity

Figure S14. XPS spectra of PEG-N-F-SiO₂ NPs with different surface PEG densities

Figure S15. Fluorescence image of droplets stabilized by PEG-N-F-SiO₂ NPs with high conjugation density (with line scan profile) where the disperse phase contained streptavidin-FITC

Figure S16. Consistent conjugation densities of molecules on the surface of $\text{NH}_2\text{-F-SiO}_2$ NPs

Table S1. Detailed reaction conditions for the surface conjugation of NPs

<i>Conjugated product</i>	<i>NPs to be conjugated</i>	<i>Conjugating agent</i>
fluo-N-F-SiO ₂ NPs (Figure 2a)	NH ₂ -F-SiO ₂ NPs (with low surface amine density)	50 mg/mL FITC in DMF
F-SiO ₂ NPs (Figure 2b)	F-SiO ₂ NPs (nothing was conjugated in this case)	50 mg/mL FITC in DMF
RB-N-F-SiO ₂ NPs (Figure S8)	NH ₂ -F-SiO ₂ NPs (with low surface amine density)	50 mg/mL RBITC in DMF
Biotin-N-F-SiO ₂ NPs (Figure 4)	NH ₂ -F-SiO ₂ NPs (both with low and high surface amine density)	50 mg/mL biotin-NHS in DMF
PEG-N-F-SiO ₂ NPs (Figure 5)	NH ₂ -F-SiO ₂ NPs (both with low and high surface amine density)	50 mg/mL mPEG-ITC in DMF

Table S2. Compositions of the continuous phase and the disperse phase for droplet generation experiments.

<i>Droplet sample</i>	<i>Continuous phase</i>	<i>Dispersed phase</i>	<i>Removing excess NPs in the continuous phase?</i>
Figures 2c and 3b	fluo-N-F-SiO ₂ NPs	DI water	Yes
Figure 4c	Biotin-N-F-SiO ₂ NPs	DI water	No
Figure 5d	NH ₂ -F-SiO ₂ NPs	20 µg/mL streptavidin-FITC in DI water	No
Figure 5e	PEG-N-F-SiO ₂ NPs	20 µg/mL streptavidin-FITC in DI water	No
Figure S1	F-SiO ₂ NPs synthesized in small scale	DI water	No
Figure S3	F-SiO ₂ NPs or NH ₂ -F-SiO ₂ NPs	DI water	No
Figure S4	F-SiO ₂ NPs	Specified in Figure S4a	Yes
Figure S6	F-SiO ₂ NPs (from scheme in Figure 2b)	DI water	Yes
Figure S9	RB _{ads} -F-SiO ₂ NPs	DI water	Yes
Figure S10	A mixture of F-SiO ₂ NPs and NH ₂ -F-SiO ₂ NPs	DI water	Yes

Figure S1. Optical image showing uniform aqueous drops generated using a continuous phase containing 1.5% (wt/wt) F-SiO₂ NPs in HFE-7500. These NPs were stored for 6 months after small-scale synthesis. This result indicates that the synthesized NPs were compatible with storage for at least 6 months before being used for the generation of drops.



200 μm

Figure S2. XPS spectrum of NH₂-F-SiO₂ NPs with initial [APTES] = 2.02 mM. A decrease in initial [APTES] led to a smaller N peak at binding energy of ~400 eV.

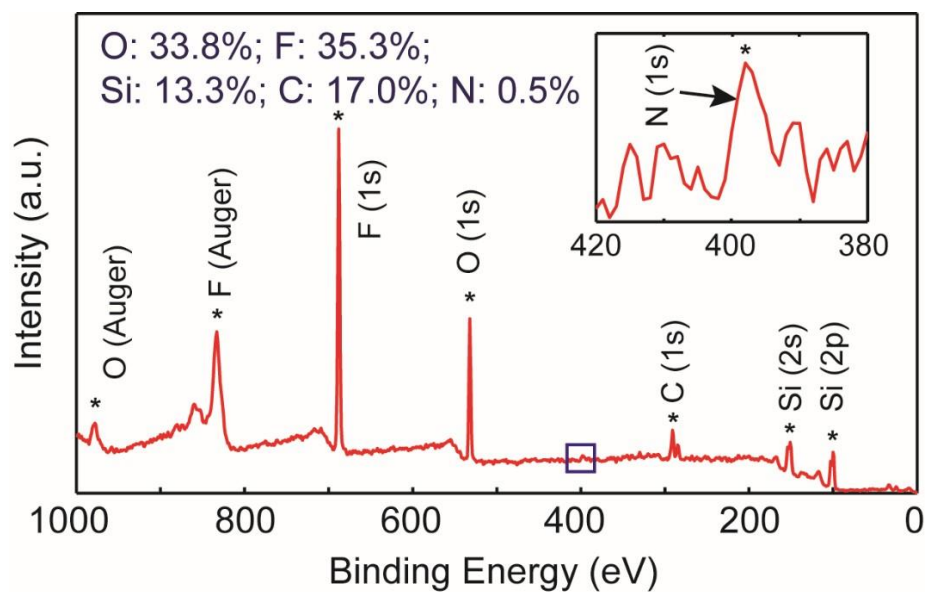


Figure S3. AES spectra of 2 μm F-SiO₂ MPs (blue), 2 μm NH₂-F-SiO₂ MPs (red) and sample substrate (Si wafer, green). Insets: SEM images of F-SiO₂ MPs and NH₂-F-SiO₂ MPs, respectively. The blue and red spots are the detection regions from which AES signals were collected. The detection regions were randomly selected on individual particle with a size of approximately 10 nm in diameter. Both nitrogen peak (~400 eV) and fluorine peak (~680 eV) were found on a single NH₂-F-SiO₂ particle, indicating the presence of both amine and fluoroalkyl groups on the same NH₂-F-SiO₂ particle. In the case of F-SiO₂ particle, however, nitrogen peak was not observed, indicating the absence of amine groups. These results confirmed the di-functionality of our synthesized NH₂-F-SiO₂ particles.

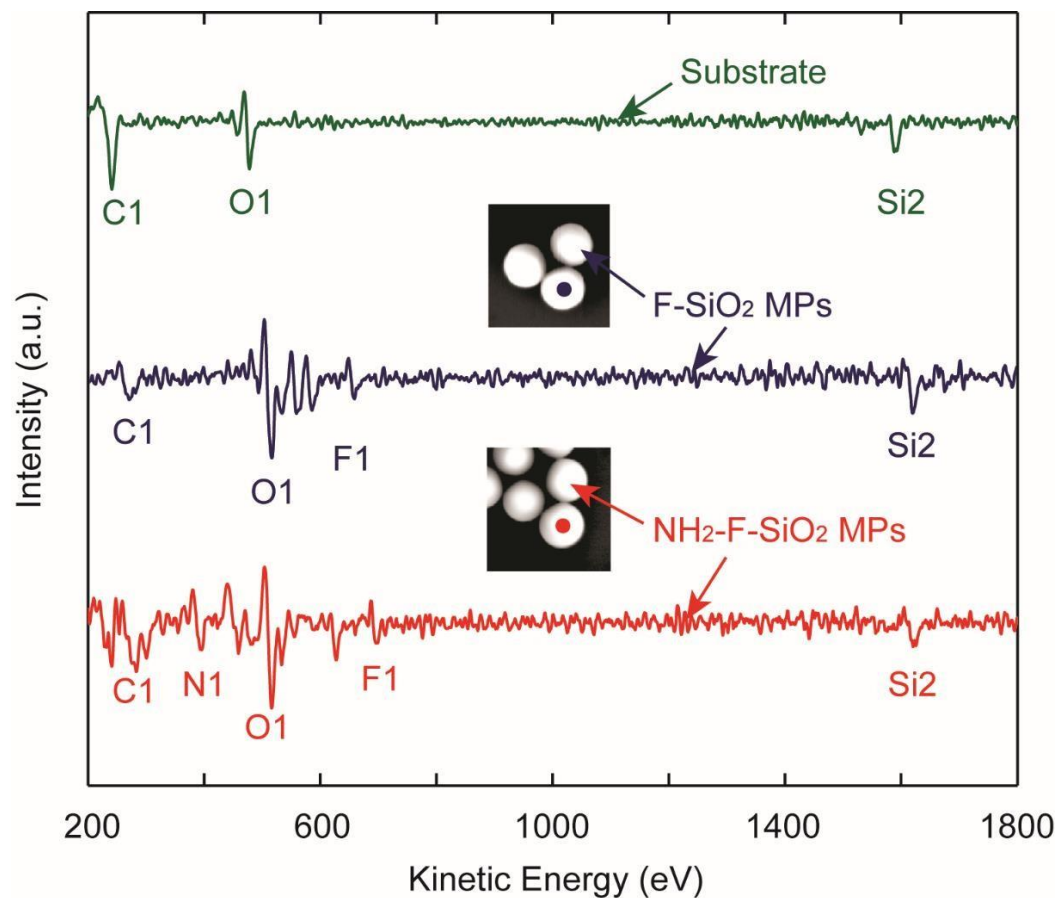


Table S3. Estimation of ratio between amine and fluoroalkyl groups on NH₂-F-SiO₂ NPs

NH₂-F-SiO₂ NPs with an initial [APTES] of:	Number of N atoms in an amine group	Number of F atoms in a fluoroalkyl group used in our work	%N : %F from XPS	Number of amine group: Number of fluoroalkyl group
101 mM	1	13	2.3% : 22.2% (from Figure 1c)	1.35:1
2.02 mM	1	13	0.5% : 35.3% (from Figure S2)	0.18:1

Figure S4. Optical images of aqueous drops after reinjection into 30 μm -tall PDMS channel. These drops were stabilized by (a) F-SiO₂ NPs and (b) NH₂-F-SiO₂ NPs, respectively. These results demonstrate droplet stability under typical manipulation conditions in droplet microfluidics.

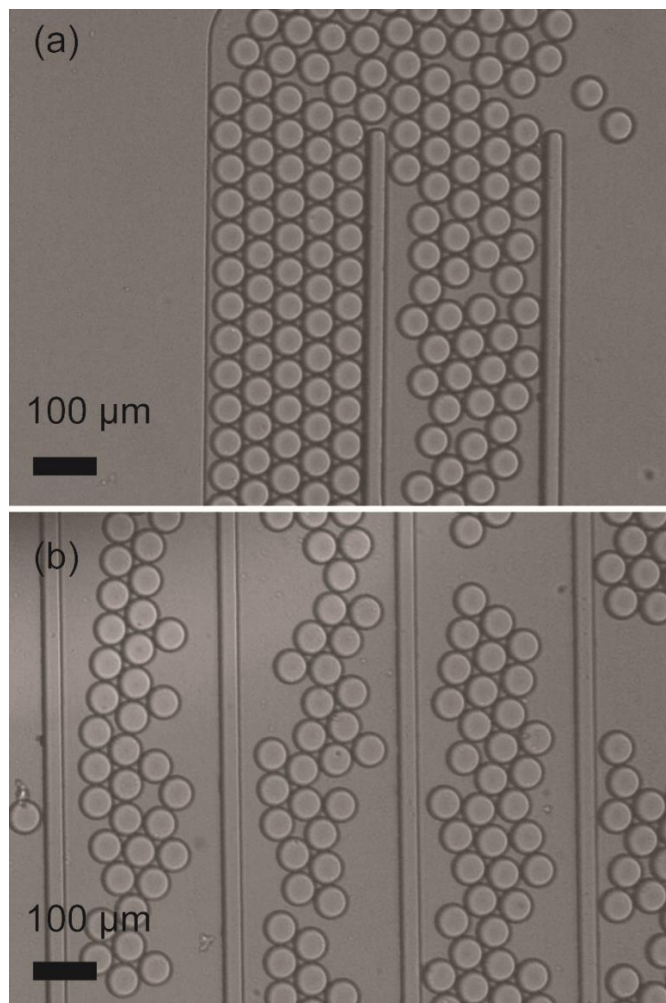




Figure S5. F-SiO₂ NPs synthesized in large scale prevent resorufin leakage. Leakage of resorufin among droplets was tested following our published work.¹ (a) Scheme showing the composition of positive and negative droplets. (b) Fluorescence images of droplet mixture before (t=5 min, top row) and after 3 hrs of incubation (t=180 min, bottom row) at room temperature. These droplets were stabilized by F-SiO₂ NPs synthesized in large scale. The positive and negative drops were mixed at 1:1 ratio at t=0. In the figure, the left column shows the fluorescence of fluorescein and the right column shows the fluorescence of resorufin. Fluorescein is the label to identify positive drops. (c) Bar charts showing fluorescence intensity of resorufin from the droplet mixture at t=5 min and t=180 min respectively, where (i, blue charts) are for positive drops and (ii, red charts) are for negative drops. The fluorescence intensity values were normalized by taking the ratio of fluorescence intensity between the resorufin and fluorescein of the same drop. For both positive and negative drops, the normalized intensity values did not change. This result indicates that the particles synthesized in large scale effectively prevented resorufin leakage from positive drops to negative drops.

(a) **Positive Droplet** **Negative Droplet**

[Resorufin] = 44 μ M \gg [Resorufin] = 8.8 μ M
[Fluorescein] = 10 μ M \gg [Fluorescein] = 2 μ M

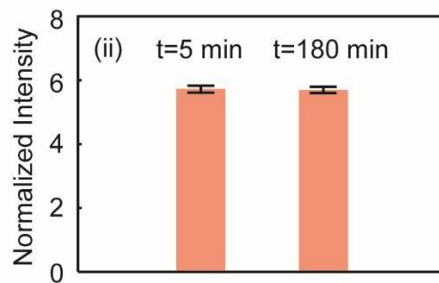
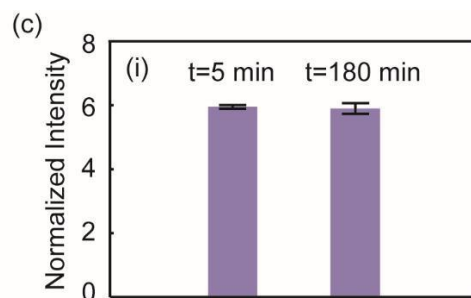
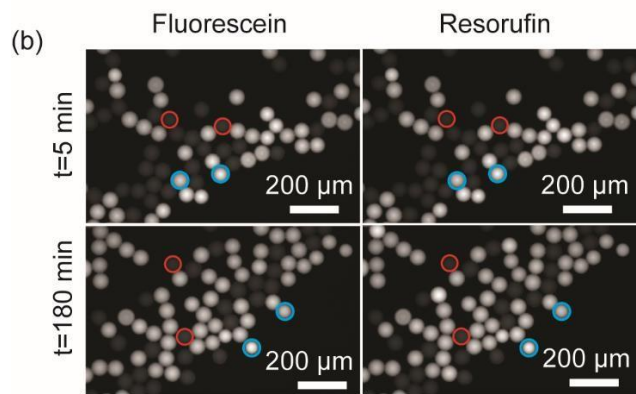


Figure S6. $\text{NH}_2\text{-F-SiO}_2$ NPs synthesized in large scale prevent resorufin leakage. Leakage of resorufin among droplets was tested following our published work.¹ (a) Scheme showing the composition of positive and negative droplets. (b) Fluorescence image of droplet mixture after 3 hrs of incubation at room temperature. These droplets were stabilized by $\text{NH}_2\text{-F-SiO}_2$ NPs synthesized in large scale. The positive and negative drops were mixed at 1:1 ratio at $t=0$. The contrast of these raw images were adjusted to show the boundaries of negative drops. After 3 hours of incubation, the fluorescence intensity of negative drops were almost the same as that in the continuous phase. This result indicates that $\text{NH}_2\text{-F-SiO}_2$ NPs effectively prevented resorufin leakage from positive drops to negative drops.

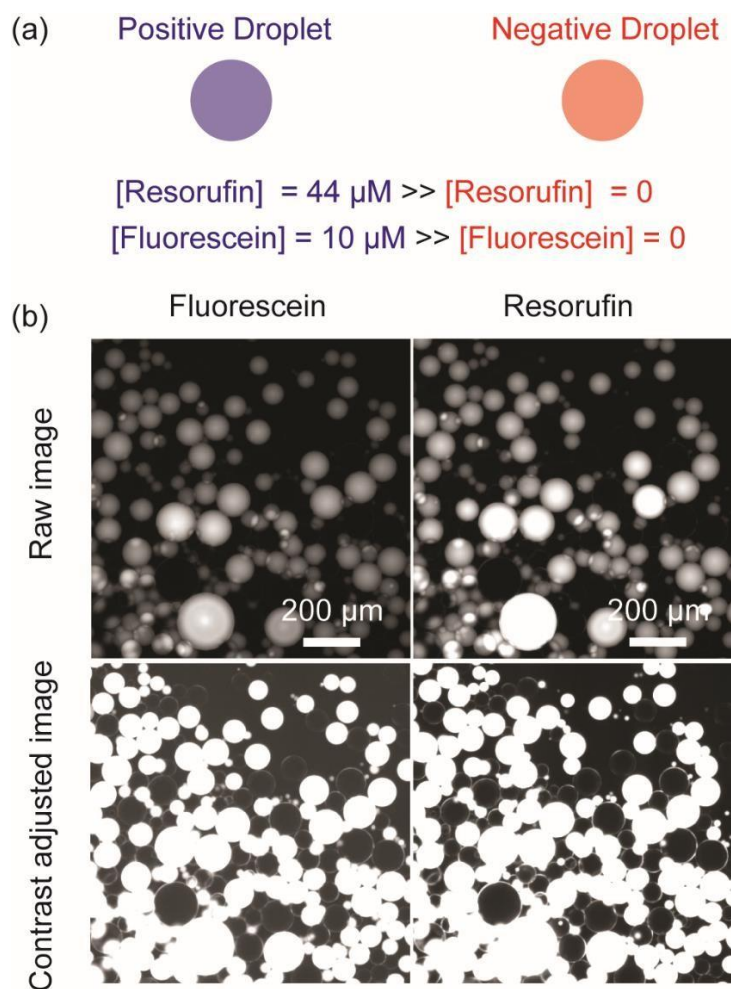


Figure S7. Fluorescence images showing the growth of *E. coli* expressing Green fluorescence Protein (“GFP *E. coli*”) inside droplets stabilized by F-SiO₂ NPs and NH₂-F-SiO₂ NPs, respectively. The droplets were produced by vortex-mixing the aqueous phase containing the cells and the continuous phase containing the nanoparticles. A few droplets containing GFP *E. Coli* were indicated by red arrows. In both cases, the cells proliferated inside the droplets from t=20 min to 210 min, indicated by an increase in the number of fluorescent dots (which correspond to cells) per droplet that contained a cell. This result suggests the two types of NPs have comparable biocompatibility with GFP *E. coli* .

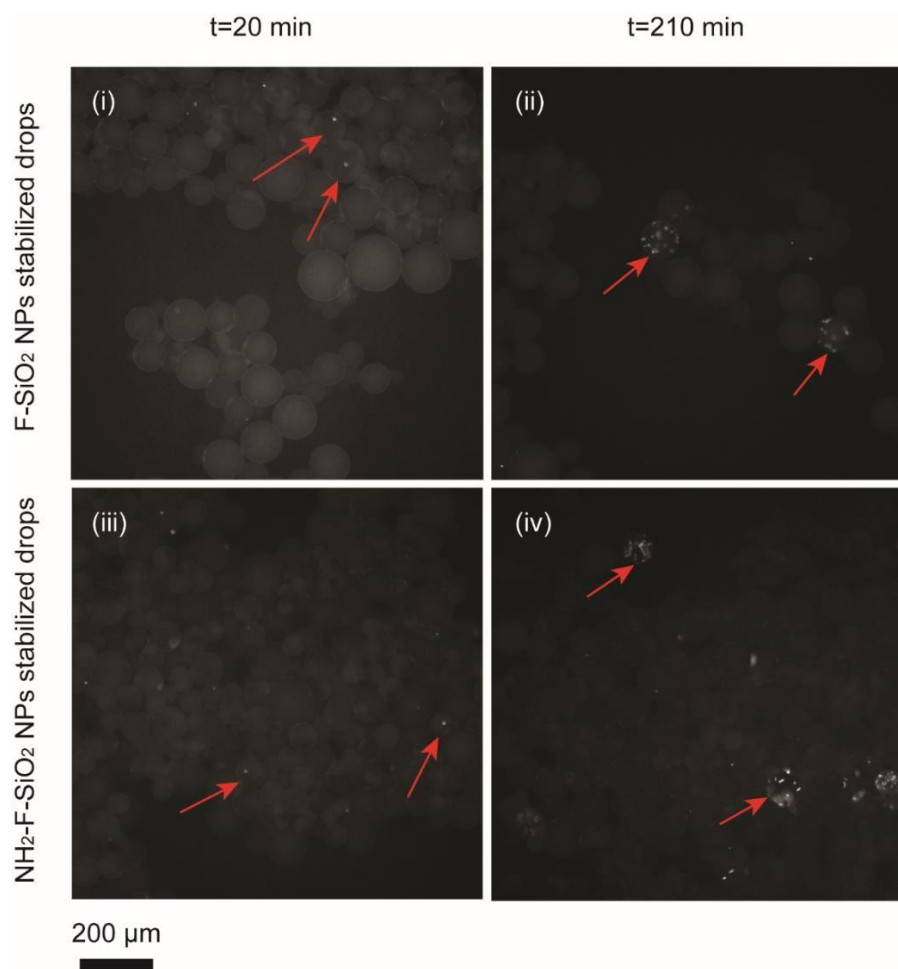


Figure S8. Bar charts showing the optical density at 600 nm (OD_{600}) for different *E. coli* K-12 (ATCC 25922) samples at (a) $t=4$ hours and (b) $t=8$ hours, respectively. The OD_{600} at $t=0$ was about 0.1 for all cases. For each OD_{600} value, three measurements were taken. For samples without droplets, at each time point 5 μL of the sample was taken out for OD_{600} measurement. For droplet samples, at each time point, 20 μL of emulsion droplets were transferred to an Eppendorf tube containing 100 μL mineral oil. The resulting mixture was swirled gently to merge all droplets into a single aqueous phase. Then 5 μL of the sample was extracted from the merged aqueous phase for OD_{600} measurement. At both time points, the OD_{600} of cells grown in $\text{NH}_2\text{-F-SiO}_2$ NPs-stabilized droplets was comparable with the other three samples, which were known to be biocompatible. This result indicates that $\text{NH}_2\text{-F-SiO}_2$ NPs are biocompatible with the growth of this type of *E. Coli*.

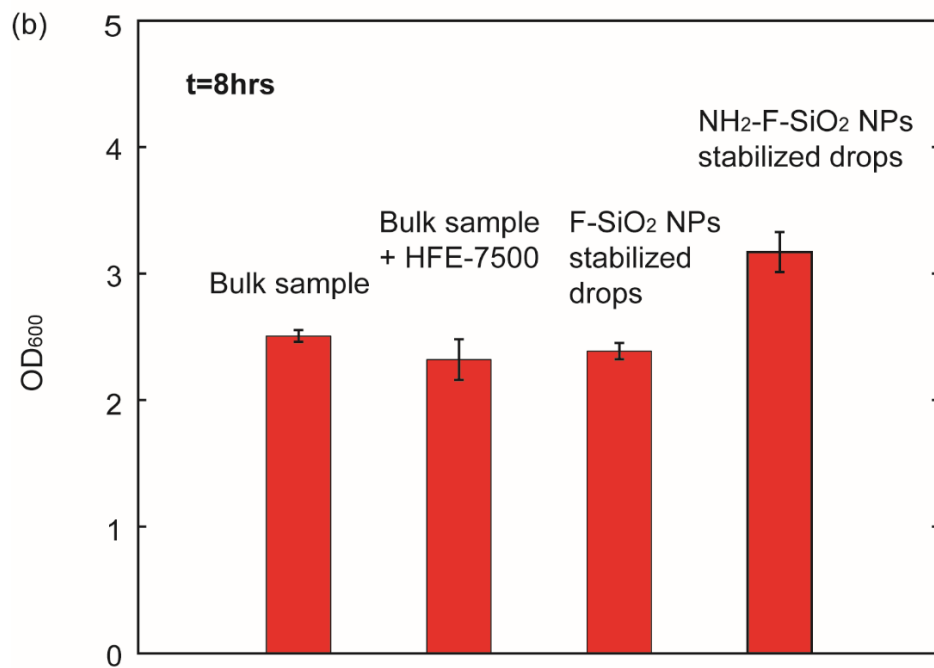
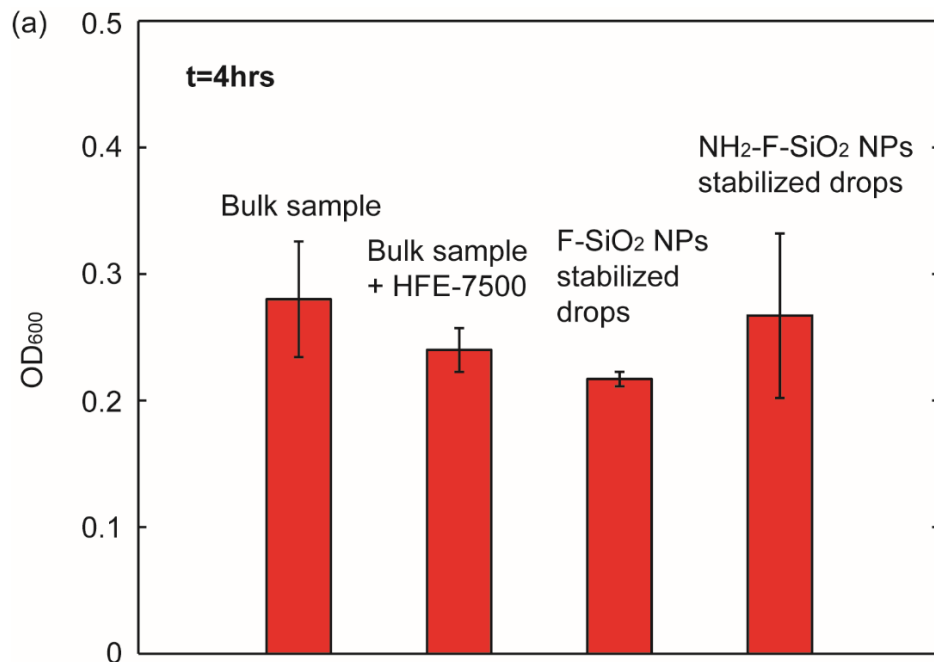


Figure S9. Fluorescence image showing aqueous drops stabilized by NPs synthesized from scheme b in Figure 2 of the main text. This image is acquired from the same sample as that in Figure 2d (inset on the right with blue arrow) but at a larger field of view. These drops were non-fluorescent with very low signal-to-noise ratio in fluorescence intensities, as shown in the blue curve in Figure 2d of the main text.

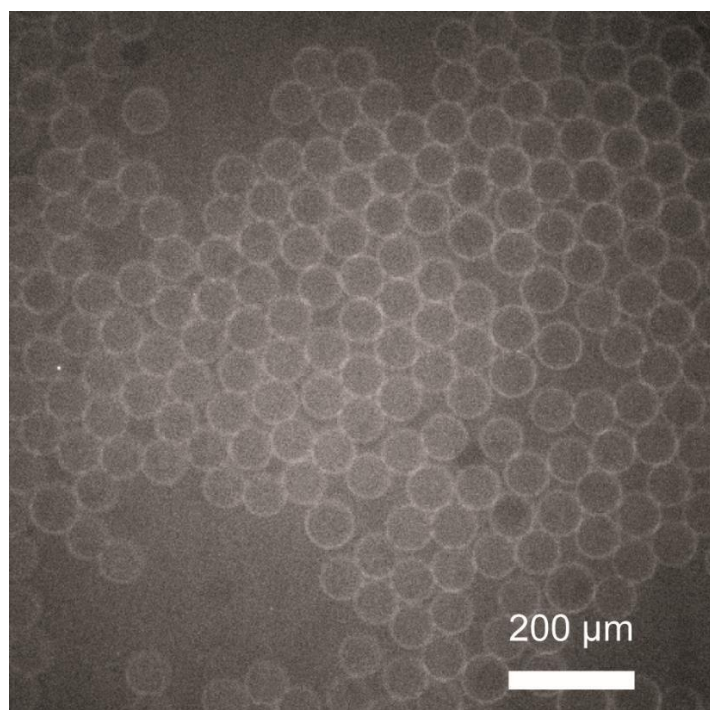


Figure S10. Fluorescein cannot be physically adsorbed on F-SiO₂ NPs. (a) Fluorescence image of aqueous drops stabilized by NH₂-F-SiO₂ NPs after these NPs were pre-incubated with excess solid fluorescein in HFE-7500. Excess solid fluorescein (10 mg) was added to 1 mL 1.5% (wt/wt) NH₂-F-SiO₂ NPs in HFE-7500 under sonication. The resulting mixture was filtered by a syringe filter (pore size: 5 μm) to remove undispersed fluorescein solid. The filtrate was collected in an Eppendorf tube. (b) Line scan on fluorescence intensity across a representative drop shown in (a) (as indicated by red arrow). The fluorescence intensity values were normalized to that in the continuous phase. The normalized intensity was much higher than the background and the intensity was the highest at the center of the drop. This profile indicates that fluorescein molecules adsorbed into NPs partitioned into the aqueous phase rather than remaining in the NPs. We speculate that some undissolved fluorescein fine powder also passed through the syringe filter and partitioned into dispersed phase after droplet formation. This may lead to the high fluorescence intensities of the resulting drops. Note that in (a), the image contrast was enhanced to highlight the intensity from the drops.

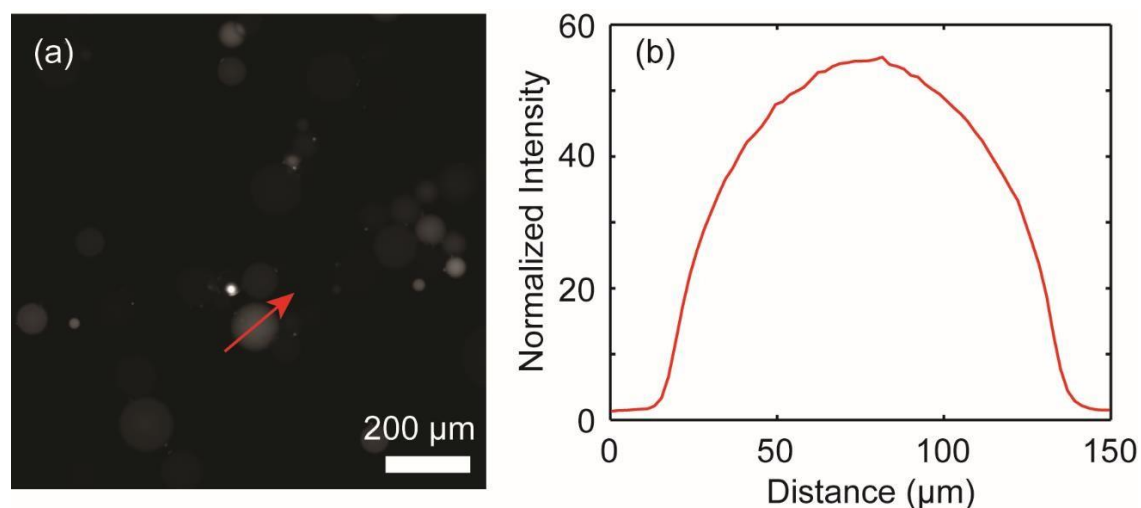


Figure S11. Covalent conjugation of Rhodamine B on $\text{NH}_2\text{-F-SiO}_2$ NPs. (a) Fluorescence image of aqueous drops stabilized by RB-N-F-SiO₂ NPs after removing excess NPs in the continuous phase. (b) Line-scan profile on fluorescence intensity across a representative drop shown in (a) (as indicated by red arrow). The fluorescence intensity values were normalized to that in the continuous phase. The presence of fluorescent rims indicates that Rhodamine B did not partition into the dispersed phase and remain preferentially adsorbed on the NPs.

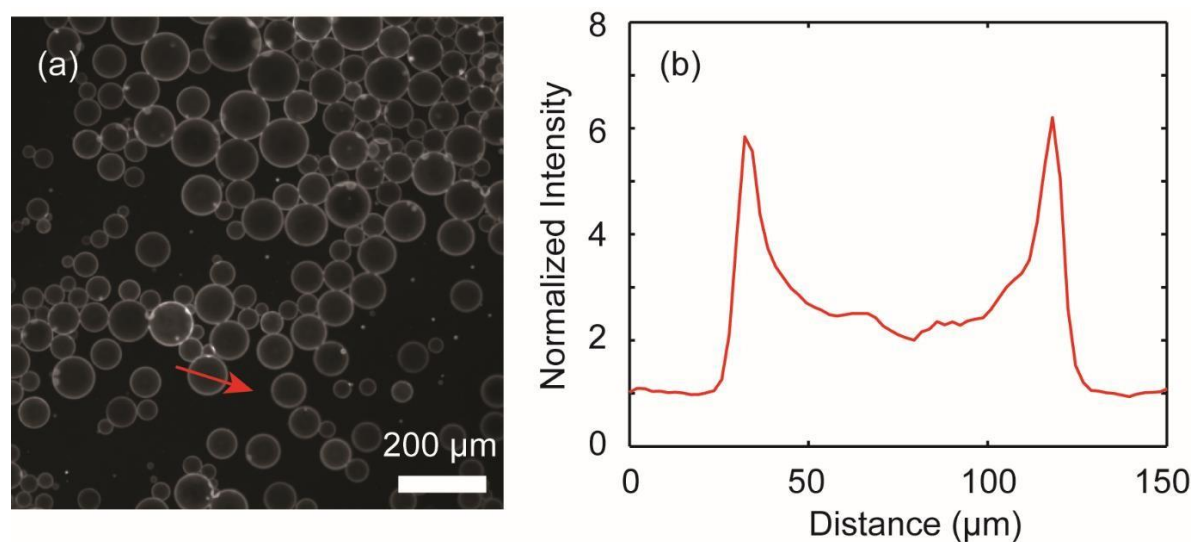


Figure S12. Rhodamine B molecules physically adsorbed onto NPs did not partition into either the dispersed phase or continuous phase containing neat HFE-7500. Fluorescence images showing aqueous drops stabilized by $\text{RB}_{\text{ads}}\text{-F-SiO}_2$ NPs (a) before and (b) after incubation in neat HFE-7500 for 3 hours. $\text{NH}_2\text{-F-SiO}_2$ NPs were pre-incubated with excess solid rhodamine B in HFE-7500. Excess solid rhodamine B (10 mg) was added to 1 mL 1.5% (wt/wt) $\text{NH}_2\text{-F-SiO}_2$ NPs in HFE-7500 under sonication. The resulting mixture was filtered by a syringe filter (pore size: $5\mu\text{m}$) to remove undispersed fluorescein solid. The filtrate was collected in an Eppendorf tube. F-SiO_2 NPs gave the same results as $\text{NH}_2\text{-F-SiO}_2$ NPs. (c) Line-scan profiles on fluorescence intensity across representative drops shown in a (indicated by blue arrow) and b (indicated by red arrow). The fluorescence intensity values were normalized to that in the continuous phase. The fluorescence intensity distribution did not show significant change after 3 hours of incubation, indicating Rhodamine B molecules did not partition into either the dispersed phase or continuous phase containing neat HFE-7500.

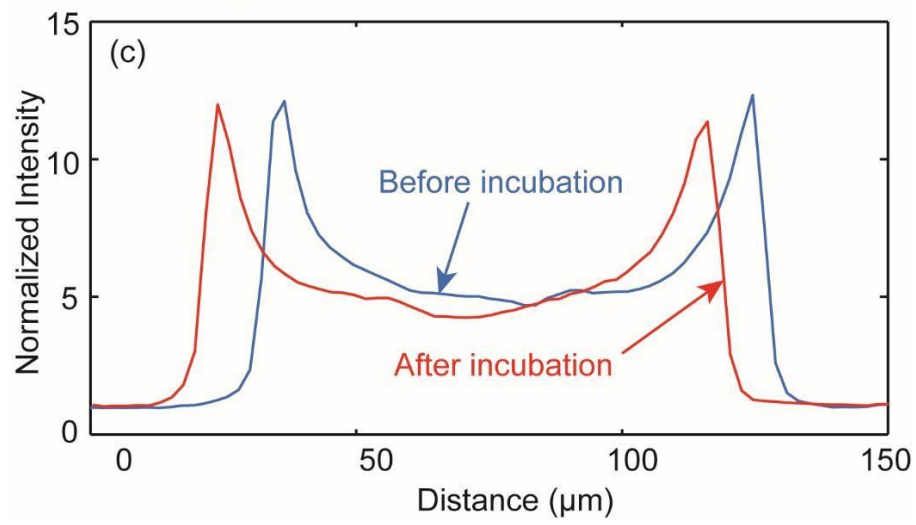
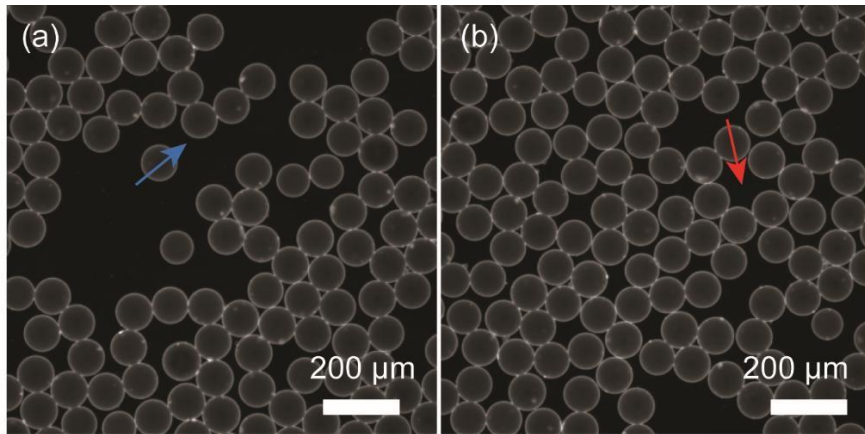


Figure S13. Plot showing the correlation between average fluorescence intensity of aqueous drops and the percentage of fluorescent NPs (fluo-N-F-SiO₂ NPs) in the NPs mixture before droplet generation. The NPs mixture contained non-fluorescent NPs (NH₂-F-SiO₂ NPs) and fluorescent NPs (fluo-N-F-SiO₂ NPs) mixed at different ratios while the total [NPs] was fixed at 1.5% (wt/wt) in HFE-7500. The droplets were generated from a flow-focusing device. The drops had a diameter of ~80 μm. For imaging, we fixed the focus at the top plane of the drops, and only the fluorescence signal from the central region of the droplet was counted to determine the average fluorescence intensity value (i.e., without counting the fluorescence signals from rim). All fluorescent intensity values were normalized to the value when the drops were stabilized by 100% fluorescent NPs. The height of the error bars represents two standard deviations of the normalized intensity obtained from ~250 data points.

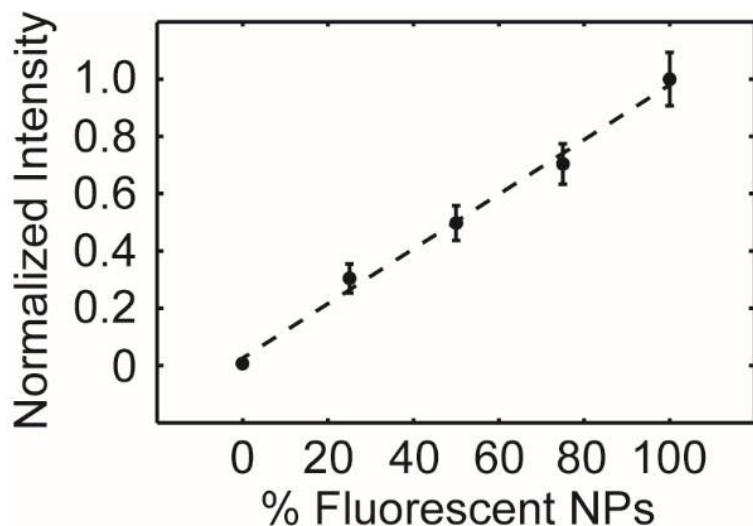


Figure S14. XPS spectra of PEG-N-F-SiO₂ NPs with different PEG densities on NPs surface. An increased PEG density was indicated by an increase of oxygen-to-fluorine content ratio and decreased dispersibility in HFE-7500.

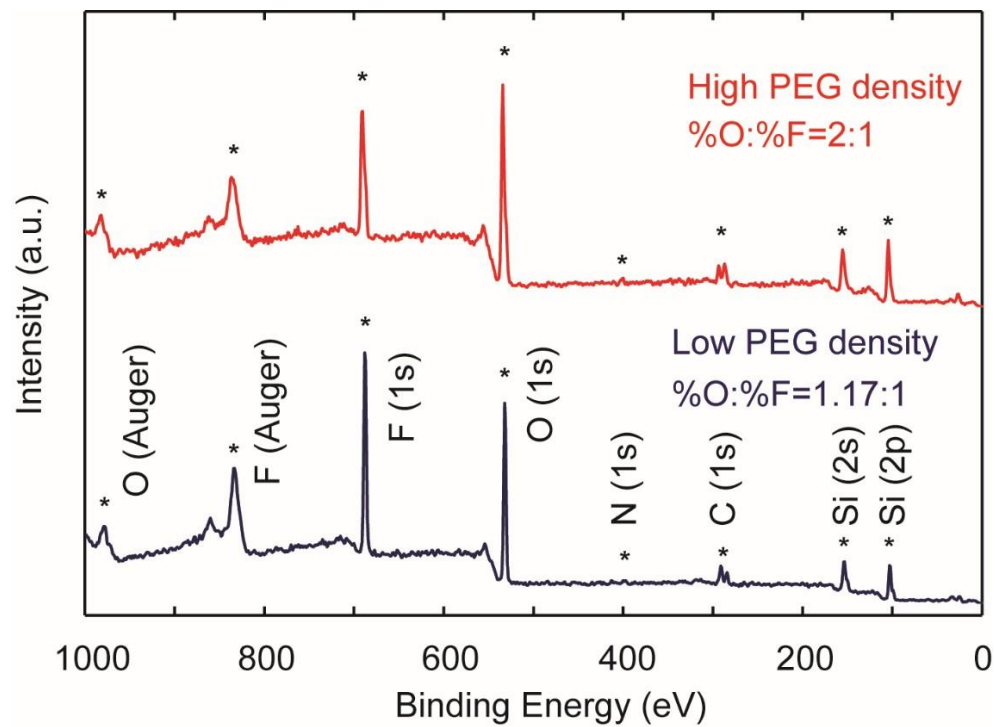


Figure S15. (a) Fluorescence image of drops stabilized by PEG-N-F-SiO₂ NPs synthesized from conjugating mPEG-ITC with NH₂-F-SiO₂ NPs with initial [APTES]= 101 mM. The dispersed phase contained 20 μg/mL streptavidin-FITC. (b) Line-scan profile on fluorescence intensity across a representative drop shown in a (as indicated by red arrow). The fluorescence intensity values were normalized to that in the continuous phase. The absence of fluorescent rims indicated that high PEG density at droplet interface prevented adsorption of streptavidin-FITC.

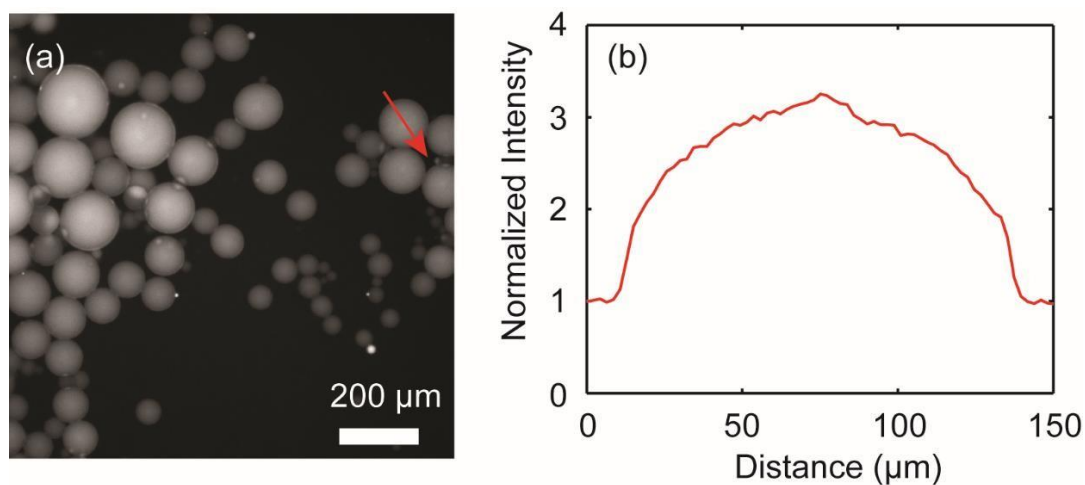
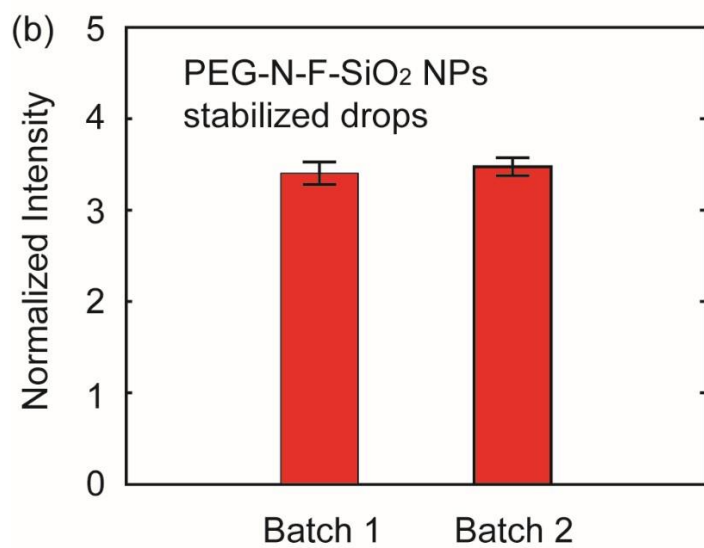
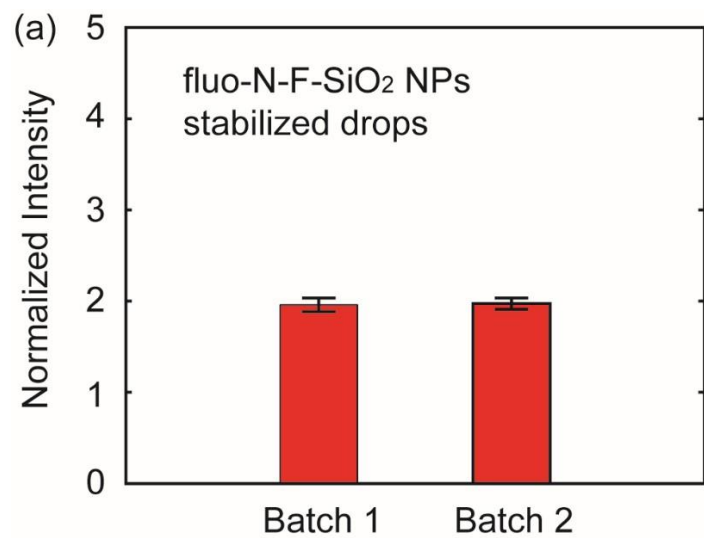


Figure S16. Bar charts showing consistency on conjugation density of both (a) fluorescent molecules and (b) polymers on $\text{NH}_2\text{-F-SiO}_2$ NPs. (a) Conjugation density of fluorescein on $\text{NH}_2\text{-F-SiO}_2$ NPs was examined by measuring the fluorescence intensity of fluo-N-F-SiO₂ NPs stabilized drops dispersed in neat HFE-7500 imaged using a fluorescence camera under fixed experimental and imaging settings. The fluorescence intensity was normalized to that in the continuous phase. (b) Conjugation density of PEG on was examined by measuring the fluorescence intensity of PEG-N-F-SiO₂ NPs-stabilized drops containing 0.1 mg/mL streptavidin-FITC dispersed in neat HFE-7500. The fluorescence intensity was also normalized to that in the continuous phase. For imaging, we fixed the focus at the top plane of the drops, and only the fluorescence signal from the central region of the droplet was counted to determine the average fluorescence intensity value (i.e., without counting the fluorescence signals from rim). In both cases, the small standard deviation (<5%) indicated consistent conjugation density of molecules from particle to particle within the same batch. The similar mean and standard deviation values between two batches indicated small batch-to-batch variation on conjugation densities. The mean and standard deviations represented in the bar charts were calculated from the measurement of 200 drops.



References

1. M. Pan, F. Lyu and S. K. Y. Tang, *Anal. Chem.*, 2015, **87**, 7938-7943.